Measuring correlations of cold atom systems using multiple quantum probes

Michael Streif,[1,2,*] Andreas Buchleitner,[2] Dieter Jaksch,[1,3] and Jordi Mur-Petit[1,†]

[1] *Clarendon Laboratory, University of Oxford, Parks Road, Oxford OX1 3PU, United Kingdom*
[2] *Physikalisches Institut, Albert-Ludwigs-Universität Freiburg, Hermann-Herder-Straße 3, 79104 Freiburg, Germany*
[3] *Centre for Quantum Technologies, National University of Singapore, 3 Science Drive 2, 117543, Singapore*

(Dated: October 11, 2016)

We present a non-destructive method to probe a complex quantum system using multiple impurity atoms as quantum probes. Our protocol provides access to different equilibrium properties of the system by changing its coupling to the probes. In particular, we show that measurements with two probes reveal the system's non-local two-point density correlations, for probe-system contact interactions. We illustrate our findings with analytic and numerical calculations for the Bose-Hubbard model in the weakly and strongly-interacting regimes, in conditions relevant to ongoing experiments in cold atom systems.

PACS numbers: 05.70.Ln, 67.85.-d 03.67.Ac
Keywords: quantum probing; strongly-correlated materials; non-equilibrium dynamics

I. INTRODUCTION

Different phases of matter are fundamentally associated with different correlations among their constituents. These correlations can be encoded in various observables. For example, the ground state of a one-dimensional, single-component Fermi gas has the same density profile as a one-dimensional system of strongly repulsive bosons (Tonks-Girardeau gas), while their momentum distributions are markedly different [1]. This stems from the fact that the momentum distribution contains further information on the two-particle correlations, which also affect other observables such as the excitation spectrum or the structure factor of quantum systems [2, 3]. While traditionally one could only access these properties via bulk measurements, e.g., neutron scattering off liquid helium, the advent of setups based on cold atoms in optical lattices has opened up new possibilities. For example, the measurement of local two-particle correlations in a one-dimensional gas of bosonic atoms for various interatomic (repulsive) interaction strengths was found [4] in excellent agreement with theoretical calculations [5–7]. Measurements of the momentum distribution [8] and non-local density-density correlation function [9] of one-dimensional bosons in a periodic potential have also been performed, and agree with theoretical findings [8, 10]. More recently, N_p-point non-local correlation functions up to $N_p = 10$ between two quasi-one-dimensional Bose gases, were measured by matter wave interferometry [11]. These results underpin the necessity to account for conserved quantities in the description of the non-equilibrium evolution of quantum systems [12–16].

Common to all these experiments is that they use destructive measurements to study the quantum systems, most frequently the time-of-flight technique where the trapping potential is switched off and the system allowed to expand before light absorption images are recorded. Based on the development of new measurement and control methods, such as the quantum gas microscope (which enables access to quantum lattice systems with single-site resolution) [17, 18], an alternative approach is advancing which considers the use of other quantum objects, such as photons, single atoms or ions [19–29], as non-destructive quantum probes of many-body quantum systems.

The idea of using single quantum probes —which often are equipped with the simplest possible internal quantum structure of a qubit— has been implemented to infer diverse properties of the host substrate, from Fröhlich polarons, to work statistics and quantum phase transitions, to the Efimov effect, and more [30–41]. Yet it is clear that a single qubit probe in general cannot suffice to map out the host's characteristic properties exhaustively, since the probe-system coupling and the thus defined local density of states will generally limit the probe's diagnostic horizon to a finite subset of the system's Hilbert space. It is therefore natural to seek a systematic generalization of the quantum probe approach to larger numbers of probes, such as to complement the finite diagnostic power of a single probe, e.g., by directly monitoring spatial correlations.

In our present contribution, we make a first step in this direction by considering two impurities embedded into a host bosonic gas [42]. Specifically, we show that the coherence of a two-probe density matrix enables to access the two-point correlation function of a strongly-correlated quantum system in a non-destructive way. We start in Sec. II with a general presentation of our two-probe protocol. In Sec. III we study a specific model of bosonic particles in a lattice, the Bose-Hubbard model (BHM), and show that our protocol enables to determine the average system density as well as the two-point density-density correlation function, both in the superfluid as well as the insulating phases of the BHM. Fi-

* michael.streif@physics.ox.ac.uk
† jordi.murpetit@physics.ox.ac.uk

nally, in section IV, we conclude with a summary of our findings and an outlook.

II. TWO-PROBE PROBING PROTOCOL

We consider a quantum system, S, coupled to two probes, which we label as L (for left) and R (right). The Hamiltonian of the composite system can be written as

$$\begin{aligned}\hat{H}_{\rm tot} =&\hat{H}_S\otimes\mathbb{1}_L\otimes\mathbb{1}_R+\mathbb{1}_S\otimes\hat{H}_L\otimes\mathbb{1}_R\\&+\mathbb{1}_S\otimes\mathbb{1}_L\otimes\hat{H}_R+\hat{H}_{\rm int}\,,\end{aligned}\tag{1}$$

where $\hat{H}_S$ is the Hamiltonian of the system and acts on the Hilbert space $\mathcal{H}_S$, $\hat{H}_\alpha$ ($\alpha = L, R$) is the Hamiltonian of the left (right) probe acting on its corresponding Hilbert space $\mathcal{H}_\alpha$, and $\hat{H}_{\rm int}$ is the interaction Hamiltonian between the system and the two impurities and therefore acts on $\mathcal{H}_{\rm tot} = \mathcal{H}_S\otimes\mathcal{H}_L\otimes\mathcal{H}_R$.

We model the probes as two-level systems (qubits), and couple them separately to the system, so that the interaction Hamiltonian reads

$$\begin{aligned}\hat{H}_{\rm int} =& \hat{V}_{SL}\otimes\left(g_{L0}\left|0\right\rangle_L\left\langle 0\right|_L+g_{L1}\left|1\right\rangle_L\left\langle 1\right|_L\right)\otimes\mathbb{1}_R\\&+\hat{V}_{SR}\otimes\mathbb{1}_L\otimes\left(g_{R0}\left|0\right\rangle_R\left\langle 0\right|_R+g_{R1}\left|1\right\rangle_R\left\langle 1\right|_R\right).\end{aligned}\tag{2}$$

Here, we have indicated the internal states of each probe qubit by $\left|0\right\rangle_\alpha, \left|1\right\rangle_\alpha$, respectively, and the parameters $g_{\alpha q}$ describe the interaction between the system and qubit $\alpha = L, R$ when in state $q = \left|0\right\rangle, \left|1\right\rangle$.

Our probing protocol starts with the qubits uncoupled from the system, $g_{\alpha q}(t = 0) = 0$. The compound initial state reads $\hat{\rho}_{\rm tot}(t = 0) = \hat{\rho}_S\otimes\left|\Phi_+\right\rangle\left\langle\Phi_+\right|$, i.e., with the two qubits not entangled with the system, and prepared in the Bell state $\left|\Phi_+\right\rangle = \left(\left|00\right\rangle+\left|11\right\rangle\right)/\sqrt{2}$, with the usual notation $\left|00\right\rangle = \left|0\right\rangle_L\otimes\left|0\right\rangle_R$ and similarly for $\left|11\right\rangle$. This entangled state can be prepared from both qubits initially in the ground state $\left|0\right\rangle$ and then subjected to a Hadamard gate acting on the left qubit followed by a controlled-NOT gate (with the left qubit as control and the right as target) [43].

At time $t = 0$, a unitary non-equilibrium evolution is driven by changing the coupling of one of the internal states of the qubits with the system, e.g., by using a Feshbach resonance. For concreteness, we set $g_{L0}(t) = g_{R0}(t) \equiv g(t) = 1$ for $t > 0$, while keeping $g_{L1}(t) = g_{R1}(t) = 0$. The state of the composite system then evolves under the time evolution operator $\hat{U}(t) = \hat{\mathcal{T}}e^{-\frac{\rm i}{\hbar}\int_0^t dt'\hat{H}_{\rm tot}(t')}$, where $\hat{\mathcal{T}}$ is the time-ordering operator, so that after a time t the composite system is in the state $\hat{\rho}_{\rm tot}(t) = \hat{U}(t)\hat{\rho}_{\rm tot}(0)\hat{U}^\dagger(t)$. A trace over the system degrees of freedom yields the reduced density matrix operator of the two qubits, $\hat{\rho}_{\rm Q}(t) = {\rm Tr}_S(\hat{\rho}_{\rm tot}(t))$. We focus our interest on the non-diagonal coherence element, whose time evolution can be expressed as $\langle 11|\hat{\rho}_{\rm Q}(t)|00\rangle = \frac{1}{4}{\rm e}^{-\frac{\rm i}{\hbar}t\Delta}\zeta(t)$. Here, the exponential factor accounts for the free evolution in terms of the energy splitting between the internal states of the two probes, $\Delta = E_{|11\rangle} - E_{|00\rangle}$; without loss of generality, we set this energy difference to zero, i.e. $\Delta = 0$. The function $\zeta(t)$ characterizes the coherence element's time dependence due to the qubits' coupling to the system; we will refer to it as the coherence function. Note that $\zeta(t)$ will generally depend on the distance between the probes, $\zeta(t) = \zeta(t;\Delta c)$ [cf. Fig. 1], which we will indicate explicitly where necessary.

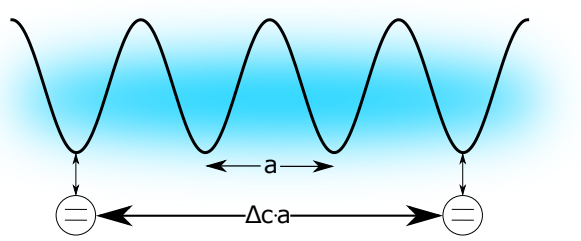

FIG. 1. A schematic representation of a Bose gas (blue shade) in an optical lattice (black line). Two ancillary two-level quantum systems (circles) are coupled to the Bose gas at distinct sites of the lattice, separated a distance Δc in units of the lattice constant a.

The moments of the interaction Hamiltonian determine the derivatives of this coherence function [39]. For example,

$$\left.\frac{{\rm d}\zeta(t)}{dt}\right|_{t=0} = \frac{\rm i}{\hbar}\left\langle\hat{H}_{\rm int}\right\rangle\,,\tag{3}$$

$$\left.\frac{{\rm d}^2\zeta(t)}{{\rm dt}^2}\right|_{t=0} = -\frac{1}{\hbar^2}\left\langle\hat{H}^2_{\rm int}\right\rangle\,,\tag{4}$$

where the expectation values on the right hand sides are calculated with $\hat{\rho}_{\rm tot}(t)$. It follows that measurements of $\zeta(t)$ permit to access several equilibrium expectation values of the system. These expectation values can be related to observables of interest by a suitable choice of the interaction between probes and system. Below, we show that, in particular, for contact probe-system interactions, measurements of the coherence function provide a way to determine the density [Eq. (9)] and the two-point density correlation function [Eq. (10)] of the host substrate.

Representing the internal state of each qubit as a spin operator, and using the Pauli spin matrices, σ_i ($i = x, y, z$), the real and imaginary parts of $\zeta(t)$ can be written

$${\rm Re}(\zeta(t)) = \frac{1}{2}\langle\hat{\sigma}_x\otimes\hat{\sigma}_x-\hat{\sigma}_y\otimes\hat{\sigma}_y\rangle_t\tag{5}$$

$${\rm Im}(\zeta(t)) = \frac{1}{2}\langle\hat{\sigma}_x\otimes\hat{\sigma}_y+\hat{\sigma}_y\otimes\hat{\sigma}_x\rangle_t,\tag{6}$$

where the bracket $\langle\cdot\rangle_t$ represents a trace over $\hat{\rho}_Q(t)$. Thus, $\zeta(t)$ can be experimentally determined by measuring the two-qubit correlation functions which enter Eqs. (5)-(6). Alternatively, one can express $\zeta(t)$ in the Bell basis as ${\rm Re}(\zeta(t)) =$

$2\,(\rho_{Q,++}(t)-\rho_{Q,--}(t))$, $\mathrm{Im}(\zeta(t)) = 4\,\mathrm{Im}\,(\rho_{Q,+-}(t))$, with $\rho_{Q,++}(t) = \langle\Phi_+|\hat{\rho}_Q(t)|\Phi_+\rangle$ and analogously for $\rho_{Q,--}$ and $\rho_{Q,+-}$, with $|\Phi_-\rangle = (|00\rangle - |11\rangle)/\sqrt{2}$. It follows that $\zeta(t)$ can also be determined with Bell-state measurements.

III. APPLICATION TO THE BOSE-HUBBARD MODEL

We now apply the protocol described in Sec. II to the case of N cold bosonic atoms loaded into the lowest energy band of an optical lattice with M sites, described by the Bose-Hubbard Hamiltonian [44, 45]

$$\hat{H}_S = -J\sum_{\langle i,j\rangle}\hat{a}_i^\dagger\hat{a}_j + \frac{U}{2}\sum_{i=1}^{M}\hat{a}_i^\dagger\hat{a}_i^\dagger\hat{a}_i\hat{a}_i + \mu\sum_{i=1}^{M}\hat{a}_i^\dagger\hat{a}_i\,. \quad (7)$$

The operator $\hat{a}_i^\dagger$ ($\hat{a}_i$) creates (annihilates) a boson at a lattice site $i = 1,\ldots,M$, the index $\langle i,j\rangle$ indicates summation over nearest neighbour pairs, and the parameters U, J and μ are the on-site interaction energy, the hopping energy and the chemical potential, respectively. We are interested in the translationally invariant system, i.e., in the limit $\{N\to\infty,\, M\to\infty\}$ with fixed average density $n = N/M$.

We now account for both probe impurities by a coupling mediated via a contact density-density interaction potential,

$$\hat{V}_{S\alpha} = \int \mathrm{d}\boldsymbol{x}\, n_\alpha(\boldsymbol{x})\hat{\Psi}^\dagger(\boldsymbol{x})\hat{\Psi}(\boldsymbol{x})\,, \qquad \alpha = L, R \quad (8)$$

where $\hat{\Psi}(\boldsymbol{x}) = \sum_j w_j(\boldsymbol{x})\hat{a}_j$ is the bosonic field annihilation operator of the system, with $w_j(\boldsymbol{x})$ the lowest energy Wannier function at the lattice site $j = 1,\ldots,M$, and $n_\alpha(\boldsymbol{x})$ the density of qubit α at position $\boldsymbol{x}$. Assuming that both impurities are strongly localized at distinct lattice sites (j_L and j_R), we find that they interact with the Wannier function of that very site only. Thus, the interaction term can be written in terms of the boson number operators at these sites, $\hat{V}_{S\alpha} = \eta_\alpha\hat{a}_{j_\alpha}^\dagger\hat{a}_{j_\alpha}$, the parameter $\eta_\alpha = J\int \mathrm{d}\boldsymbol{x}|w_\alpha(\boldsymbol{x})|^2 n_\alpha(\boldsymbol{x})$ being a measure of the interaction strength between the bosons and the qubit at site j_α. For simplicity, we assume that the local interaction strength at both probe locations are identical, i.e., $\eta_L = \eta_R \equiv \eta$.

Substitution of Eq. (8) into Eq. (2), together with Eq. (3), yields the expectation value of the interaction's contribution to the total Hamiltonian which, due to the specific form of $V_{S\alpha}$, is equal to the bosonic density $\hat{\rho}(j) = \hat{a}_j^\dagger\hat{a}_j$ at site j:

$$2\overline{\rho} = \langle\hat{\rho}(j) + \hat{\rho}(j+\Delta c)\rangle = \frac{\hbar}{\mathrm{i}\eta}\frac{\mathrm{d}\zeta(t;\Delta c)}{dt}\bigg|_{t=0}\,, \quad (9)$$

For the first equality, we used that, for translationally invariant systems, $\langle\hat{\rho}(j)\rangle = \langle\hat{\rho}(j+\Delta c)\rangle \equiv \overline{\rho}$, with the integer $\Delta c = j_R - j_L$ the distance between the two qubits in units of the lattice constant a, see Fig. 1. (In an experiment, this can be accomplished by trapping the two qubits in a separate optical lattice formed by crossing two laser beams; the inter-qubit distance Δc can then be precisely tuned by changing the angle between the propagation directions of the beams, see e.g., [46].)

Similarly, using Eq. (4), we find the bosonic density-density correlation function $\mathrm{Cor}(\Delta c) = \langle\hat{\rho}(j)\hat{\rho}(j+\Delta c)\rangle$ in terms of the qubits' coherence function:

$$\langle[\hat{\rho}(j) + \hat{\rho}(j+\Delta c)]^2\rangle = -\frac{\hbar^2}{\eta^2}\frac{\mathrm{d}^2\zeta(t;\Delta c)}{dt^2}\bigg|_{t=0}\,. \quad (10)$$

Again, given the system's translational invariance, $\langle\hat{\rho}(j)^2\rangle = \langle\hat{\rho}(j+\Delta c)^2\rangle$, the last expression can be rewritten as

$$\mathrm{Cor}(\Delta c) = \frac{\hbar^2}{2\eta^2}\frac{\mathrm{d}^2}{dt^2}\left[\frac{1}{2}\zeta(t;\Delta c=0) - \zeta(t;\Delta c)\right]\bigg|_{t=0}\,. \quad (11)$$

This result implies that measurements of the qubits' coherence function $\zeta(t)$ provide access to the system's density-density correlation function. We remark that this result depends on the qubits-system coupling, Eq. (8), but not on the specific form of the system Hamiltonian $\hat{H}_S$ beyond its translational invariance. In the following sections, we assess the experimental feasibility of our protocol by simulating the outcome of the protocol in both the superfluid ($U/J \ll 1$) and the insulating ($U/J \gg 1$) phases of the one-dimensional Bose-Hubbard model, and comparing them with exact results for $\mathrm{Cor}(\Delta c)$ in both limits.

A. Weak interactions: Superfluid phase

In the regime of weak interactions ($U/J \ll 1$), we can use Bogoliubov theory [47] to calculate both the coherence function $\zeta(t)$ and the density-density correlation function $\mathrm{Cor}(\Delta c)$ analytically (see also [28, 48]). We start from the Bose-Hubbard Hamiltonian (7) for a one-dimensional system of homogeneous density n. We first transform the annihilation operators from the site basis, $\hat{a}_i$, to the momentum basis, $\hat{b}_k = (M)^{-1/2}\sum_j \hat{a}_j e^{\mathrm{i}kaj}$, and similarly for the creation operator $\hat{b}_k^\dagger$. A Bogoliubov transformation to quasiparticle operators, $\hat{d}_k = u_k\hat{b}_k + v_k\hat{b}_{-k}^\dagger$, brings the system Hamiltonian into the diagonal form $\hat{H}_S = \sum_k \hbar\omega_k\hat{d}_k^\dagger\hat{d}_k$, with $\hat{d}_k$ ($\hat{d}_k^\dagger$) the annihilation (creation) operator of Bogoliubov quasiparticles of quasi-momentum k, and $\omega_k = \sqrt{\epsilon_k(\epsilon_k + 2U\overline{\rho})}$ the quasiparticle dispersion relation in terms of the single-particle energies $\epsilon_k = 2J(1-\cos(ka))$, with a the lattice constant and $\overline{\rho}$ the bosonic density [49].

With this transformation, we rewrite the density matrix of the lattice bosons by expressing the bosonic oper-

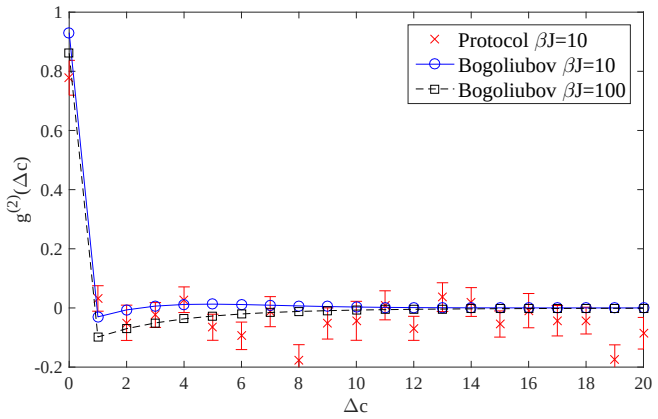

FIG. 2. *Weak interactions.* Normalized correlation function obtained with Eq. (11) simulating $N_{\rm exp} = 10^4$ experiments (crosses), compared with the analytic results Eq. (13) (lines with symbols), for a system initially at equilibrium at inverse temperature $\beta J = 10$ and $\beta J = 100$. Other parameters used are $\eta = 0.4J$ and $U/J = 0.1$.

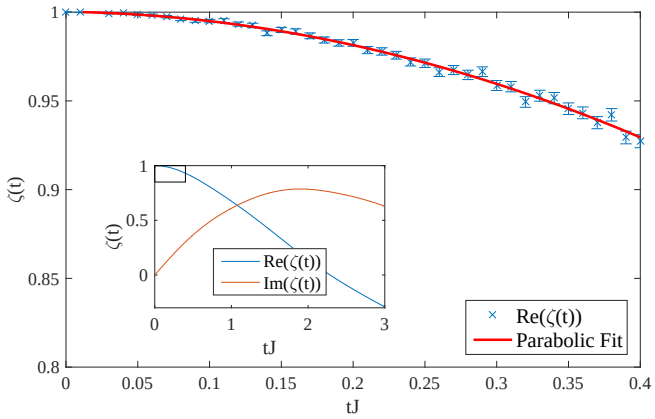

FIG. 3. Real part of the coherence function with added Gaussian noise (symbols) and a parabolic fit (solid line). *(Inset)* Real (blue) and imaginary (red) parts of $\zeta(t)$, Eq. (16), for the case $\Delta c = 5$. In this Figure, we used a system with $M = 1000$ lattice sites and $N = 1000$ bosons; and therefore an average density $\overline{\rho} = 1$. The system is initially in a thermal state with $\beta J = 10$; other parameters as in Fig. 2.

ators in terms of Bogoliubov quasiparticle operators

$$\hat{\rho}_j = \hat{a}_j^\dagger \hat{a}_j = \frac{1}{M}\sum_{k,k'} \hat{b}_k^\dagger \hat{b}_{k'} e^{\mathrm{i}kaj} e^{-\mathrm{i}k'aj}$$
$$= \overline{\rho} + \frac{\sqrt{N_0}}{M}\sum_k \sqrt{\frac{\epsilon_k}{\omega_k}}\left(d_k^\dagger e^{\mathrm{i}kaj} + d_k e^{-\mathrm{i}kaj}\right). \quad (12)$$

In the second line, we applied Bogoliubov's approximation, i.e., we assume that the occupation of $k \neq 0$ modes is small $[(N-N_0)/N \ll 1]$, and neglect terms of quadratic (or higher) order in quasiparticle operators [47, 49]. By inserting Eq. (12) into the definition of the two-point density correlation function, we reach the following analytic expression valid in the weakly-interacting limit

$$\mathrm{Cor}(\Delta c) = \overline{\rho}^2 + \frac{\overline{\rho}}{M}\sum_k \frac{\epsilon_k}{\omega_k}(2n_k^{\rm th}+1)\cos\left(ka\Delta c\right), \quad (13)$$

where we evaluated the occupations of the Bogoliubov modes in a thermal state, $\langle \hat{d}_k^\dagger \hat{d}_k\rangle = n_k^{\rm th} = 1/(e^{\beta\hbar\omega_k}-1)$, with β the inverse temperature, and we dropped the anomalous averages $\langle \hat{d}_k \hat{d}_{-k}\rangle$ as they are negligible at the low temperatures where the Bogoliubov approximation applies [50]. At zero temperature ($\beta \to \infty$), Eq. (13) satisfies the sum rule established in Ref. [51] for density-density correlations in the ground state, which re-expresses the sum rule relating the dynamic structure factor with the static structure factor, which in turn is sensitive to two-body interactions in bosonic lattice systems [52].

Based on Eq. (13), we plot in Fig. 2 the normalized second order correlation function

$$g^{(2)}(\Delta c) = \frac{\langle\hat{\rho}(0)\hat{\rho}(\Delta c)\rangle - \langle\hat{\rho}(0)\rangle\langle\hat{\rho}(\Delta c)\rangle}{\langle\hat{\rho}(0)\rangle^2}, \quad (14)$$

as a function of the inter-probe distance Δc for different temperatures. We see that, for all temperatures, the correlation vanishes for distances beyond a few lattice sites, which agrees with the picture that, in the non-interacting limit, the system is effectively described by a product of on-site coherent states so that $\langle\hat{\rho}(0)\hat{\rho}(\Delta c)\rangle = \langle\hat{\rho}(0)\rangle\langle\hat{\rho}(\Delta c)\rangle$ [53]. Weakly-interacting homogeneous one-dimensional Bose gases also converge to this limit fairly quickly [54].

We proceed now to compare these analytic calculations with the estimation by means of the coherence function $\zeta(t)$. To evaluate the right-hand side of Eq. (11), we rewrite the system-qubit interaction Hamiltonian in terms of Bogoliubov operators,

$$\hat{V} = \hat{V}_{SL} + \hat{V}_{SR} = 2\overline{\rho}\eta + \sum_k \left(\eta_k^\star \hat{d}_k^\dagger + \eta_k \hat{d}_k\right), \quad (15)$$

where $\eta_k = \eta\sqrt{n\epsilon_k/M\omega_k}(e^{-\mathrm{i}kaj_L} + e^{-\mathrm{i}kaj_R})$ is the coupling strength of the qubits with the Bogoliubov mode of quasi-momentum k. Substituting these expressions into $\hat{H}_{\rm int}$ allows us to calculate analytically the time evolution of the composite system, and therefore to determine the coherence function $\zeta(t)$. Full details of the derivation are contained in Appendix A [see also [42]], here we quote only the final result

$$\zeta(t) = e^{2\mathrm{i}\eta\overline{\rho}t}\exp\left[-\mathrm{i}\sum_k \frac{|\eta_k|^2}{\omega_k^2}[\omega_k t - \sin(\omega_k t)]\right]$$
$$\times \exp\left[\sum_k\left(-2\frac{|\eta_k|^2}{\omega_k^2}\sin^2\frac{\omega_k t}{2}\coth\frac{\beta\omega_k}{2}\right)\right]. \quad (16)$$

In an experiment, the coherence function $\zeta(t)$ can only be measured at discrete times, t_r. In addition, for

each time t_r, the expectation value defining $\zeta(t_r)$ is obtained upon accumulation of repeated measurements of the qubits' state, with individual measurement outcomes exhibiting quantum (shot) noise. To simulate this unavoidable spread of experimental measurement events, and to estimate how many measurements one would need for their statistical average to converge to the expectation value, we follow the scheme of Ref. [38] and add Gaussian noise to the calculated values of $\zeta(t_r)$; see Appendix B for detail on how to determine the corresponding variance. As one would do in an experiment, to reduce the ensuing uncertainty in $\zeta(t_r)$, we repeat the simulated experiment a number $N_{\rm exp}$ of times and average over all outcomes, for each inter-probe distance Δc. The values of $\zeta(t_r)$ estimated in this way are presented in Fig. 3 for a system with average density $\overline{\rho} = 1$. Here, one can note that the real part of $\zeta(t)$ has a parabolic dependence on time, while the imaginary part is linear around $t = 0$. It follows that the second derivative will be real, in accordance with our expectations for the density-density correlation function, cf. Eq. (11). Thus, in practice it suffices to measure only the real part of $\zeta(t)$, Eq. (5).

Given the smooth character of $\zeta(t_r)$, we fit a quadratic polynomial through these values, which enables us to calculate the right-hand side of Eq. (11) and determine the two-point correlation function. We show the corresponding results for $\beta J = 10$ in Fig. 2, which are in fair agreement with the analytic result (13). In particular, we see that the value of $g^{(2)}(0)$ derived from the protocol shows the characteristic enhancement of the superfluid phase. Reducing the statistical uncertainty of $g^{(2)}(\Delta c)$ for $\Delta c \gg 1$ requires a relatively large number of measurements $N_{\rm exp}$, in line with previous experimental determinations of $g^{(2)}(\Delta c)$ in cold atomic setups [55, 56]. In the framework of the present two-probe protocol, these fluctuations, and correspondingly $N_{\rm exp}$, can be reduced by running in parallel an arrangement with $N_{\rm pairs}$ pairs of probes in a double-well super-lattice [57–60]; a setup with $N_{\rm pairs} = 100$ probe pairs would reach the precision shown in Fig. 2 with only 100 measurement runs.

B. Strong interactions: Insulating phase

For stronger interactions $U/J \gtrsim 1$, the correlations between the bosons in the lattice invalidate an approach based on the Bogoliubov treatment. An efficient method to deal with this situation is Tensor Network Theory (TNT), which provides numerically exact ground state properties of strongly-correlated systems, in particular of the one-dimensional BHM [61, 62]. Here, we apply this method to calculate $g^{(2)}(\Delta c)$ in the ground state of this model using the implementation Oxford TNT library [63]. As we are interested in investigating non-local correlation functions, we choose a large system with $M = 101$ lattice sites, and $\overline{\rho} = 1$ as before, and calculate $g^{(2)}(\Delta c)$ around the central lattice site so that boundary effects are negligible and the system can still be considered (approximately) translationally invariant. For the calculations presented below, we have checked that sufficient accuracy is reached bounding the site occupation to a maximum of 4 bosons per site and fixing a truncation parameter (maximum number of Schmidt coefficients) of $\chi = 100$.

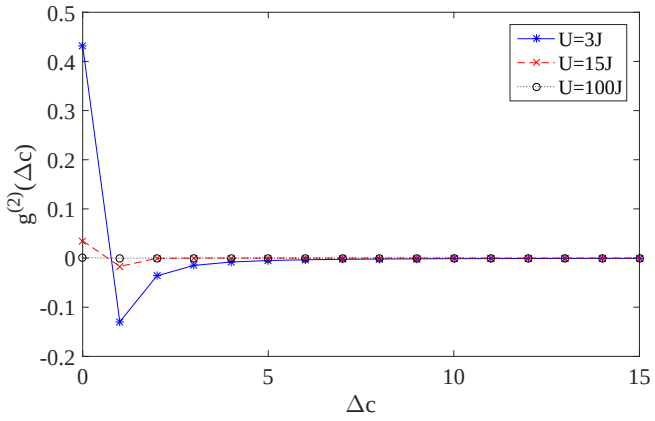

FIG. 4. Correlation function $g^{(2)}(\Delta c)$ for the ground state in the strongly-interacting regime for different interactions strengths $U/J = 3$, 15 and 100 as indicated. These points represent the numerically exact expectation values of number operator pairs, $(\langle\hat{\rho}_i\hat{\rho}_j\rangle - \langle\hat{\rho}_i\rangle\langle\hat{\rho}_j\rangle)\,/\,\langle\hat{\rho}_i\rangle^2$, from the TNT calculation.

The TNT method allows us to calculate directly the expectation values of the number operator at each lattice site, $\langle\hat{\rho}_i\rangle$, and all pairs of number operators, $\langle\hat{\rho}_i\hat{\rho}_j\rangle$. From these, we obtain directly the normalized two-point correlation function $g^{(2)}(\Delta c) = (\langle\hat{\rho}_i\hat{\rho}_{i+\Delta c}\rangle - \langle\hat{\rho}_i\rangle\langle\hat{\rho}_{i+\Delta c}\rangle)\,/\,\langle\hat{\rho}_i\rangle^2$; the results for increasing values of U/J are shown in Fig. 4. As expected, in the limit $U/J \to \infty$ we recover that $g^{(2)}(\Delta c) = 0\ \forall \Delta c$ as the ground state is a product of on-site Fock states with no density fluctuations [53, 64]. These results constitute the test-bed corresponding to the left-hand site of Eq. (11), which we will compare to the outcome of the protocol to obtain $\zeta(t)$ and its derivatives.

We calculate $\zeta(t)$ in the strongly-interacting regime in the following way: The coherence function can be written as a trace over system operators only $\zeta(t) = {\rm Tr}_S(\hat{U}_1(t)\hat{U}_0(t)\hat{\rho}_\beta)$, cf. Eq. (A1). Here, $\hat{U}_0(t)$ is the evolution operator over a time t with the initial system Hamiltonian, while $\hat{U}_1(t)$ is the evolution operator including the coupling to the qubits. For probe qubits localized at lattice sites and coupled to the bosons by contact interactions of strength η, the effect of the probe-boson coupling amounts to a local shift of the bosons' chemical potential, $\mu \to \mu - \eta$, at the sites where the probes are located. Thus, we can obtain $\zeta(t_r)$ at different time steps t_r by calculating the expectation value ${\rm Tr}_S(\hat{U}_1(t)\hat{U}_0(t)\hat{\rho}_\beta)$ with $\hat{\rho}_\beta$ the ground state of the bosonic system in a lattice with modified local potential at the probe sites.

In our numerical calculations, we take $t_r = r\Delta t$ with $\Delta t = \hbar \times 0.01/J$ and $r = 0, \ldots, 20$. As for the weakly-

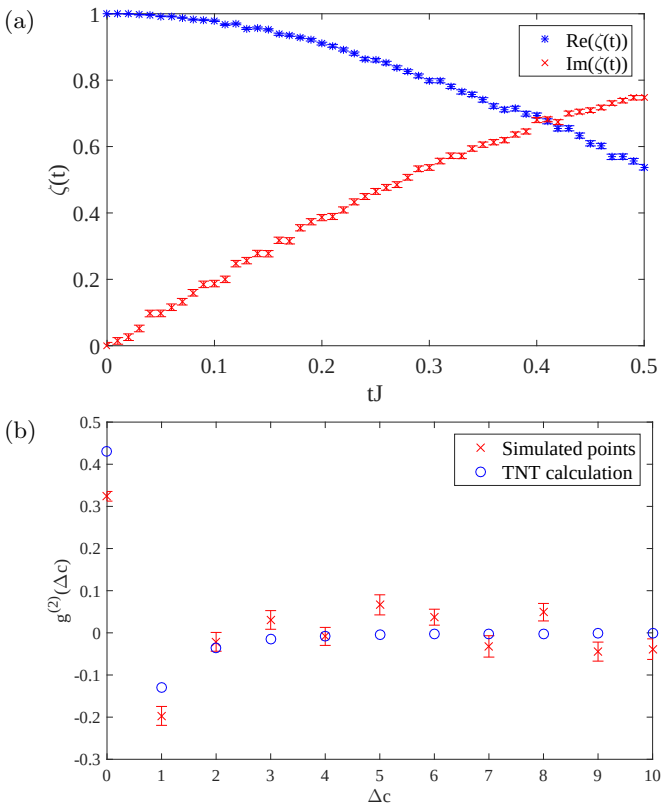

FIG. 5. *Strong interactions.* (a) Real (asterisks) and imaginary (crosses) part of the coherence function $\zeta(t)$ for $U/J = 3$. Other parameters are $\Delta c = 5$, $M = 101$, $\overline{\rho} = 1$, and $\eta = J$. (b) Normalized correlation function $g^{(2)}(\Delta c)$ for the same parameters. The results of the measurement protocol with $N_{\rm exp} = 10^4$ (crosses) agree with the numerically exact values calculated with the TNT method (circles).

interacting regime, we simulate the uncertainty in an experiment by adding noise to each simulated data point, $\zeta(t_r)$, and calculate the numerical second derivative at $t = 0$. We repeat this procedure for all integer distances between the two qubits $0 \leq \Delta c \leq 15$ ($\ll M$ to avoid boundary effects). The coherence function, $\zeta(t)$ obtained in this way is shown in Fig. 5(a). We observe that both real and imaginary parts exhibit broadly a similar behaviour to that of the weakly interacting system. However, the correlation function that one obtains from this according to Eq. (11) is notably different, as can be seen in Fig. 5(b), where we compare the value of $g^{(2)}(\Delta c)$ obtained from the coherence function by using Eq. (11) with the numerically exact values derived from the TNT ground state (these latter values are the same as those in Fig. 4 for $U/J = 3$). We see that there is a good agreement between the two calculations, as it happened in the weakly interacting regime. In particular, the estimation of the correlation function using our protocol is able to detect the reduction of $g^{(2)}(0)$ as the system gets deeper into the Mott insulating phase, $U/J \gg 1$. To illustrate this point, we show in Fig. 6 the normalized

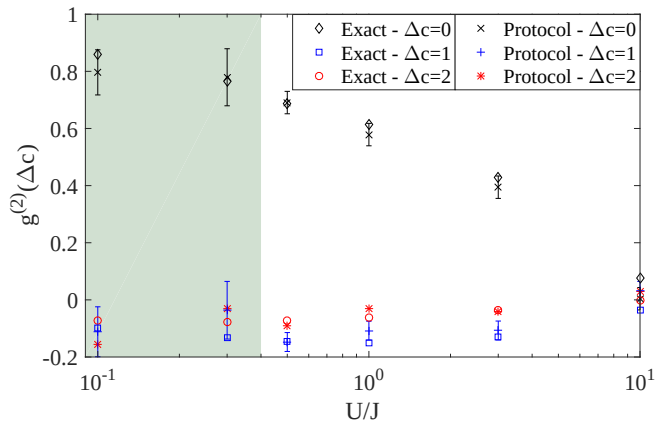

FIG. 6. Correlation function $g^{(2)}(\Delta c)$ for $\Delta c \in \{0, 1, 2\}$ and different values of U/J. Bogoliubov theory was used for $U/J \leq 0.4$ with a $\beta J = 1000$ thermal state (shaded region), and TNT for larger values of U/J. For clarity, we do not include only error bars for the $\Delta c = 2$ calculation; they are similar to those for $\Delta c = 1$.

correlation function $g^{(2)}(\Delta c)$ at selected distances Δc for different values of U/J across the Mott insulator to superfluid transition. First, we observe that the outcome of our protocol in each case is very close to the exact result (calculated with Bogoliubov theory for weak interactions and with TNT for stronger interactions). Physically, the local correlation, $g^{(2)}(0)$, decreases steadily as the repulsion between bosons increases, and vanishes in the limit $U/J \gg 1$. Correlations at larger distances are negative (meaning, it is *less* probable to find a particle at distance Δc in the actual ground state than what one would predict by relying only on the average density) and generally of smaller magnitude than the local correlation; they also vanish in the strongly-repulsive limit, as expected for a Mott insulator.

IV. SUMMARY AND OUTLOOK

In this paper, we have developed a framework to study correlation functions in cold atom systems by using multiple atomic impurities as quantum probes. We presented a protocol which is able to measure the density-density correlations of the system relying on measuring the internal states of the probes and studying one of the off-diagonal elements of the two-particle density matrix. We have shown that the results of this protocol agree with those of analytic and numerically exact calculations for a one-dimensional Bose-Hubbard model in both the weakly and strongly interacting regimes. In particular, we have shown that the protocol is able to witness the change in correlations across the superfluid to Mott insulator transition.

The framework presented here opens new possibilities for the experimental investigation of quantum many-body systems and, especially, systems of cold atoms in

optical lattices. The protocol can be extended in various ways. For example, one can consider using $N > 2$ quantum probes to determine N-point correlation functions. Another possibility lies in the freedom of choosing the kind of interaction Hamiltonian between qubits and system. By having a different kind of interaction Hamiltonian one could get access to different observables of the system. For example, by coupling the qubits to the system using Raman couplings [65], the evolution of the probes becomes sensitive to the phase of the matter wave and one could measure cross-correlation functions [66].

ACKNOWLEDGMENTS

The authors would like to thank J. J. Mendoza-Arenas, T. H. Johnson, and M. Mitchison for useful discussions. This work was supported by the EU H2020 Collaborative project QuProCS (Grant Agreement No. 641277), EU Seventh Framework Programme (FP7/2007-2013) Grant Agreement No. 319286 Q-MAC, and Erasmus Placements (M.S.). D. J. thanks the Graduate School of Excellence Material Science in Mainz for hospitality during part of this work.

Appendix A: Bogoliubov treatment of the weakly interacting system

We briefly expand on the explicit calculation of the coherence function $\zeta(t)$ for weak interactions, with the help of Bogoliubov theory, and following the procedure outlined in [38]. The first step is to introduce a set of projection operators on the Hilbert space of the two qubits,

$$\begin{aligned} \hat{\mathcal{P}}_{11} &= |11\rangle\langle 11| \,, \quad & \hat{\mathcal{P}}_{10} &= |10\rangle\langle 10| \,, \\ \hat{\mathcal{P}}_{01} &= |01\rangle\langle 01| \,, \quad & \hat{\mathcal{P}}_{00} &= |00\rangle\langle 00| \,. \end{aligned}$$

This enables us to rewrite the full Hamiltonian in a more convenient form.

$$\begin{aligned} \hat{H}_{\rm tot} = \hat{\mathcal{P}}_{11} \otimes \left(E_1 + \hat{H}_S + g_{L1}\hat{V}_{SL} + g_{R1}\hat{V}_{SR}\right) + \\ + \hat{\mathcal{P}}_{10} \otimes \left(E_2 + \hat{H}_S + g_{L1}\hat{V}_{SL} + g_{R0}\hat{V}_{SR}\right) + \\ + \hat{\mathcal{P}}_{01} \otimes \left(E_3 + \hat{H}_S + g_{L0}\hat{V}_{SL} + g_{R1}\hat{V}_{SR}\right) + \\ + \hat{\mathcal{P}}_{00} \otimes \left(E_4 + \hat{H}_S + g_{L0}\hat{V}_{SL} + g_{R0}\hat{V}_{SR}\right) \end{aligned}$$

As said in the main part, we are interested in the time evolution of the qubits only. Therefore, after calculating the time evolution of the composite system, we trace out the degrees of freedom of the bosons. After that, we concentrate on the coherence element of the two-qubit density matrix, $\langle 11|\hat{\rho}_{\rm Q}|00\rangle$. We find that the coherence function can be determined by calculating the expectation value

$$\zeta(t) = {\rm Tr}_S(\hat{U}_1(t)\hat{U}_0(t)\hat{\rho}_S) \tag{A1}$$

with the initial state of the system $\hat{\rho}_S$. In this expression

$$\hat{U}_0(t) = \hat{\mathcal{T}} \exp\left(-\frac{\rm i}{\hbar}\int_0^t {\rm dt}'\hat{H}_S\right)$$

is the time evolution operator with the unperturbed system Hamiltonian, and

$$\hat{U}_1(t) = \hat{\mathcal{T}} \exp\left(-\frac{\rm i}{\hbar}\int_0^t {\rm dt}'(\hat{H}_S + g(\hat{V}_{SL} + \hat{V}_{SR}))\right)$$

is the time evolution operator with the Hamiltonian including the coupling to the probes, where we used that $g_{L0} = g_{R0} = 1$ and $g_{L1} = g_{R1} = 0$. It is worth noting the similarity of $\zeta(t)$ with the Loschmidt echo [67, 68], which is a function that enables to characterize memory effects in the dynamics of quantum systems, see e.g. [69].

For simplicity, we change into the interaction picture, where $\hat{U}_0 = \mathbb{1}$. The remaining time evolution operator simplifies to a more convenient expression.

$$\hat{U}_1(t) = \hat{\mathcal{T}} \exp\left(-\frac{\rm i}{\hbar}\int_0^t dt'\hat{V}_{\rm int}(t')\right) .$$

Here, $\hat{V}_{\rm int}(t)$ is the interaction part of the Hamiltonian in the interaction picture,

$$\hat{V}_{\rm int}(t) = 2\overline{\rho}\eta + \sum_k \left(\eta_k^\star e^{{\rm i}\omega_k t}\hat{b}_k^\dagger + \eta_k\hat{b}_k e^{-{\rm i}\omega_k t}\right) .$$

We can simplify the expression for $\hat{U}_1$ by applying the Magnus expansion [70]. To this end, we introduce an operator $\hat{A}$ by

$$\hat{\mathcal{T}} \exp\left(-\frac{\rm i}{\hbar}\int_0^t dt'\hat{V}_{\rm int}(t')\right) = {\rm e}^{\hat{A}} .$$

This operator can be expressed as a sum of operators $\hat{A} = \sum_i \hat{A}_i$ which are related to commutators of the interaction Hamiltonian.

$$\begin{aligned} \hat{A}_1 &= -{\rm i}\int_0^t dt'\hat{V}_{\rm int}(t') \\ \hat{A}_2 &= \frac{1}{2}\int_0^t {\rm dt}'\int_0^{t'} {\rm dt}''[\hat{V}_{\rm int}(t'), \hat{V}_{\rm int}(t'')] \\ &\vdots \end{aligned}$$

Given the form of $\hat{V}_{\rm int}$ above, the commutators at different times are c-numbers, $[\hat{V}_{\rm int}(t'), \hat{V}_{\rm int}(t'')] = -2i\sum_k |\eta_k|^2 \sin(\omega_k(t'-t''))$. Therefore, all terms of the expansion beyond the second term vanish. Thus, we can write the coherence function as follows

$$\begin{aligned} \zeta(t) = e^{2{\rm i}\overline{\rho}\eta t} \exp\left[-{\rm i}\sum_k \frac{|\eta_k|^2}{\omega_k^2}[\omega_k t - \sin(\omega_k t)]\right] \\ \times {\rm Tr}\left[\exp\left\{-{\rm i}\sum_k\left(\gamma_k\hat{d}_k^\dagger + \gamma_k^\star\hat{d}_k\right)\right\}\hat{\rho}_S\right] \end{aligned} \tag{A2}$$

where we defined $\gamma_k = \frac{\eta_k^\star}{\omega_k}\left(\frac{e^{i\omega_k t}-1}{\mathrm{i}}\right)$. We are left with the task to calculate the trace over the initial state $\hat{\rho}_S$. A close investigation of this expression reveals that the operator acting on $\hat{\rho}_S$ is a displacement operator, $\hat{\mathcal{D}}(\alpha) = e^{\alpha\hat{d}^\dagger - \alpha^\star \hat{d}}$, for each Bogoliubov mode with corresponding displacement $\mathrm{i}\gamma_k$. Due to this and the commutation relations of Bogoliubov operators, $[\hat{d}_k^\dagger, \hat{d}_{k'}] = \delta_{k,k'}$, we can write the trace in the last line of Eq. (A2) as the expectation value of a product of displacement operators

$$\begin{aligned}\text{trace} &= \mathrm{Tr}\left[\prod_k \hat{\mathcal{D}}_k(\mathrm{i}\gamma_k)\hat{\rho}_\beta\right] \\ &= \sum_{\{n_k\}}\prod_k \frac{\langle\hat{\rho}_k\rangle^{n_k}}{(1+\langle\hat{\rho}_k\rangle)^{n_k+1}}\langle\{n_k\}|\prod_{k'}\hat{\mathcal{D}}_{k'}(\mathrm{i}\gamma_{k'})|\{n_k\}\rangle\,.\end{aligned}$$

Here, we have considered that initially the system is in a thermal equilibrium state at inverse temperature β, so that $\hat{\rho}_S = \exp(-\beta\hat{H}_S)/Z$, with the partition function $Z = \mathrm{Tr}[\exp(-\beta\hat{H}_S)]$, and then used the diagonal representation of the thermal state in the Fock basis.

The action of a displacement operator on a Fock state $|n\rangle$ is to generate a displaced Fock state $|n,\gamma\rangle$. The remaining overlap of two of these states can be expressed by [71]

$$\begin{aligned}&\langle n,\gamma|m,\alpha\rangle \\ &= \langle\gamma|\alpha\rangle\sqrt{\frac{n!}{m!}}(\gamma^\star-\alpha^\star)^{m-n}L_n^{m-n}[(\gamma-\alpha)(\gamma^\star-\alpha^\star)]\,,\end{aligned}$$

where $L_n^a(x)$ are the generalized Laguerre polynomials and $\langle\gamma|\alpha\rangle = \exp[-\frac{1}{2}\left(|\gamma|^2+|\alpha|^2-2\gamma^\star\alpha\right)]$ is the overlap of two coherent states. This enables us to calculate the trace as

$$\begin{aligned}\text{trace} &= \sum_{\{n_k\}}\prod_k \frac{\langle\hat{n}_k\rangle^{n_k}}{(1+\langle\hat{n}_k\rangle)^{n_k+1}}\langle\{n_k\}|\{n_k\},\{i\gamma_k\}\rangle \\ &= \prod_k\sum_{\{n_k\}}\frac{\langle\hat{n}_k\rangle^{n_k}}{(1+\langle\hat{n}_k\rangle)^{n_k+1}}e^{-\frac{1}{2}|\gamma_k|^2}L_{n_k}^0(|i\gamma_k|^2)\,.\end{aligned}$$

This expression can be simplified with the generating function of Laguerre polynomials, $\sum_{n=0}^\infty t^n L_n(x) = \frac{1}{1-t}e^{-\frac{tx}{1-t}}$ [72], which leads to

$$\text{trace} = \exp\left\{\sum_k\left[-\frac{1}{2}|\gamma_k|^2\coth\left(\frac{\beta\hbar\omega_k}{2}\right)\right]\right\},$$

where we used $\langle\hat{n}_k\rangle = 1/(\exp(\beta\hbar\omega_k)-1)$ for a thermal state. Substituting this result into Eq. (A2) provides Eq. (16).

Appendix B: Calculation of the variance

We show how to estimate the uncertainty in the measurement of $\mathrm{Re}(\zeta(t))$ due to the projection noise on the measurement of the state of the qubits. In this way, we determine the noise which has to be added to the calculated values of the coherence function to simulate the outcome of experiments.

In accordance with Eq. (5),

$$\mathrm{Re}(\zeta(t)) = \frac{1}{2}\langle\hat{\sigma}_x\otimes\hat{\sigma}_x - \hat{\sigma}_y\otimes\hat{\sigma}_y\rangle\,, \tag{B1}$$

the real part of the coherence function can be determined by measuring the expectation value of a combination of Pauli matrices on the state of the qubits. Hence, we start by calculating the variance associated with this expectation value. Introducing the shorthand notation $\hat{\sigma}_{xx} = \hat{\sigma}_x\otimes\hat{\sigma}_x$, and similarly for $\hat{\sigma}_{yy}$ and $\hat{\sigma}_{zz}$, we have

$$\mathrm{Var}(\hat{\sigma}_{xx}-\hat{\sigma}_{yy}) = \langle(\hat{\sigma}_{xx}-\hat{\sigma}_{yy})^2\rangle - \langle\hat{\sigma}_{xx}-\hat{\sigma}_{yy}\rangle^2\,.$$

The last term is directly related to the coherence function $\langle\hat{\sigma}_{xx}-\hat{\sigma}_{yy}\rangle^2 = 4\mathrm{Re}(\zeta(t))^2$, whereas the first can be calculated as follows

$$\begin{aligned}\langle(\hat{\sigma}_{xx}-\hat{\sigma}_{yy})^2\rangle &= \langle\hat{\sigma}_{xx}^2+\hat{\sigma}_{yy}^2-\hat{\sigma}_{xx}\hat{\sigma}_{yy}-\hat{\sigma}_{yy}\hat{\sigma}_{xx}\rangle \\ &= 2\langle\mathbb{1}_4+\hat{\sigma}_{zz}\rangle\end{aligned} \tag{B2}$$

where $\mathbb{1}_4$ is the 4×4 identity matrix. In the last line, we used that the Pauli matrices fulfill the algebraic relation $\hat{\sigma}_a\,\hat{\sigma}_b = \delta_{ab}\mathbb{1}_2 + \mathrm{i}\sum_{c=x,y,z}\epsilon_{abc}\,\hat{\sigma}_c$. We observe that the right-hand side of Eq. (B2) is a diagonal matrix. Since the time evolution does not affect the diagonal elements, we can evaluate this expectation value over the initial Bell state, resulting in $\langle(\hat{\sigma}_{xx}-\hat{\sigma}_{yy})^2\rangle = 4$. Thus,

$$\mathrm{Var}(\hat{\sigma}_{xx}-\hat{\sigma}_{yy}) = 4\left[1-\mathrm{Re}(\zeta(t))^2\right]\,.$$

Substituting this into Eq. (B1), it follows that the variance of the real part of the coherence function is connected to the function itself via

$$\mathrm{Var}(\mathrm{Re}(\zeta(t)) = \frac{1}{4}\mathrm{Var}(\hat{\sigma}_{xx}-\hat{\sigma}_{yy}) = 1-\mathrm{Re}(\zeta(t))^2\,.$$

For the error on the imaginary part of the coherence function, the calculation is analogous.

Having determined the variances of the real and imaginary parts of $\zeta(t)$, we simulate the uncertainty in experiments by adding Gaussian noise of zero mean and standard deviations $\sigma_{\mathrm{Re}} = \sqrt{1-\mathrm{Re}(\zeta(t))^2}$ and $\sigma_{\mathrm{Im}} = \sqrt{1-\mathrm{Im}(\zeta(t))^2}$ to the real and imaginary parts, respectively.

[1] M. A. Cazalilla, R. Citro, T. Giamarchi, E. Orignac, and M. Rigol, "One dimensional bosons: From condensed matter systems to ultracold gases," Reviews of Modern Physics **83**, 1405–1466 (2011).

[2] David Pines and Philippe Nozières, *The Theory of Quantum Liquids, vol I*, Vol. 2 vols (W. A. Benjamin, New York, 1990).

[3] Anthony J. Leggett, *Quantum liquids: Bose condensation and Cooper pairing in condensed-matter systems*, Oxford Graduate Texts (Oxford University Press, Oxford, 2006).

[4] Toshiya Kinoshita, Trevor Wenger, and David S. Weiss, "Local Pair Correlations in One-Dimensional Bose Gases," Physical Review Letters **95**, 190406 (2005).

[5] D. M. Gangardt and G. V. Shlyapnikov, "Stability and Phase Coherence of Trapped 1D Bose Gases," Physical Review Letters **90**, 010401 (2003).

[6] M. A. Cazalilla, "Differences between the Tonks regimes in the continuum and on the lattice," Physical Review A **70**, 041604 (2004).

[7] K. V. Kheruntsyan, D. M. Gangardt, P. D. Drummond, and G. V. Shlyapnikov, "Finite-temperature correlations and density profiles of an inhomogeneous interacting one-dimensional Bose gas," Physical Review A **71**, 053615 (2005).

[8] Belén Paredes, Artur Widera, Valentin Murg, Olaf Mandel, Simon Fölling, Ignacio Cirac, Gora V. Shlyapnikov, Theodor W. Hänsch, and Immanuel Bloch, "Tonks–Girardeau gas of ultracold atoms in an optical lattice," Nature **429**, 277–281 (2004).

[9] Simon Fölling, Fabrice Gerbier, Artur Widera, Olaf Mandel, Tatjana Gericke, and Immanuel Bloch, "Spatial quantum noise interferometry in expanding ultracold atom clouds," Nature **434**, 481–484 (2005).

[10] Ehud Altman, Eugene Demler, and Mikhail D Lukin, "Probing many-body states of ultracold atoms via noise correlations," Phys. Rev. A **70**, 013603 (2004).

[11] Tim Langen, Sebastian Erne, Remi Geiger, Bernhard Rauer, Thomas Schweigler, Maximilian Kuhnert, Wolfgang Rohringer, Igor E Mazets, Thomas Gasenzer, and Jörg Schmiedmayer, "Experimental observation of a generalized Gibbs ensemble." Science (New York, N.Y.) **348**, 207–11 (2015).

[12] Javier Madroñero, Alexey V. Ponomarev, Andre R.R. Carvalho, Sandro Wimberger, Carlos Viviescas, Andrey R. Kolovsky, Klaus Hornberger, Peter Schlagheck, Andreas Krug, and Andreas Buchleitner, "Quantum chaos, transport and control - in quantum optics," Adv. At. Mol. Opt. Phys. **53**, 33 (2006).

[13] Marcos Rigol, Vanja Dunjko, and Maxim Olshanii, "Thermalization and its mechanism for generic isolated quantum systems." Nature **452**, 854–8 (2008).

[14] Moritz Hiller, Hannah Venzl, Tobias Zech, Bartolmiej Oleś, Florian Mintert, and Andreas Buchleitner, "Robust states of ultracold bosons in opical lattices," J. Phys. B **45**, 095301 (2012).

[15] J.L. Birman, R.G. Nazmitdinov, and V.I. Yukalov, "Effects of symmetry breaking in finite quantum systems," Phys. Rep. **526**, 1 (2013).

[16] Johannes Freese, Boris Gutkin, and Thomas Guhr, "Spreading in integrable and non-integrable many-body systems," Physica A **461**, 683 (2016).

[17] Waseem S. Bakr, Jonathon I. Gillen, Amy Peng, Simon Fölling, and Markus Greiner, "A quantum gas microscope for detecting single atoms in a Hubbard-regime optical lattice," Nature **462**, 74–77 (2009).

[18] Jacob F. Sherson, Christof Weitenberg, Manuel Endres, Marc Cheneau, Immanuel Bloch, and Stefan Kuhr, "Single-atom-resolved fluorescence imaging of an atomic Mott insulator," Nature **467**, 68–72 (2010).

[19] Alexey V. Ponomarev, Javier Madroñero, Andrey R. Kolovsky, and Andreas Buchleitner, "Atomic current across an optical lattice," Physical Review Letters **96**, 050404 (2006).

[20] I Mekhov, Christoph Maschler, and Helmut Ritsch, "Light scattering from ultracold atoms in optical lattices as an optical probe of quantum statistics," Physical Review A **76**, 053618 (2007).

[21] Scott N. Sanders, Florian Mintert, and Eric J. Heller, "Matter wave scattering from ultracold atoms in an optical lattice," Phys. Rev. Lett. **105**, 035301 (2010).

[22] Christoph Zipkes, Stefan Palzer, Carlo Sias, and Michael Köhl, "A trapped single ion inside a Bose–Einstein condensate," Nature **464**, 388–391 (2010).

[23] Stefan Schmid, Arne Härter, and Johannes Hecker Denschlag, "Dynamics of a cold trapped ion in a Bose-Einstein condensate," Phys. Rev. Lett. **105**, 133202 (2010).

[24] Sebastian Will, Thorsten Best, Simon Braun, Ulrich Schneider, and Immanuel Bloch, "Coherent interaction of a single fermion with a small bosonic field," Phys. Rev. Lett. **106**, 115305 (2011).

[25] Stefan Hunn, Moritz Hiller, Doron Cohen, Tsampikos Kottos, and Andreas Buchleitner, "Inelastic chaotic scattering on a bose-einstein condensate," J. Phys. B **45**, 085302 (2012).

[26] Nicolas Spethmann, Farina Kindermann, Shincy John, Claudia Weber, Dieter Meschede, and Artur Widera, "Dynamics of single neutral impurity atoms immersed in an ultracold gas," Phys. Rev. Lett. **109**, 235301 (2012).

[27] Takeshi Fukuhara, Adrian Kantian, Manuel Endres, Marc Cheneau, Peter Schauß, Sebastian Hild, David Bellem, Ulrich Schollwöck, Thierry Giamarchi, Christian Gross, *et al.*, "Quantum dynamics of a mobile spin impurity," Nature Physics **9**, 235–241 (2013).

[28] Klaus Mayer, Alberto Rodriguez, and Andreas Buchleitner, "Matter-wave scattering from interacting bosons in an optical lattice," Physical Review A - Atomic, Molecular, and Optical Physics **90**, 023629 (2014).

[29] Wojciech Kozlowski, S.F. Caballero-Benitez, and I Mekhov, "Probing matter-field and atom-number correlations in optical lattices by global nondestructive addressing," Physical Review A **92**, 013613 (2015).

[30] Michael Hohmann, Farina Kindermann, Benjamin Gänger, Tobias Lausch, Daniel Mayer, Felix Schmidt, and Artur Widera, "Neutral impurities in a Bose-Einstein condensate for simulation of the Fröhlich-polaron," EPJ Quantum Technology **2**, 1–15 (2015).

[31] Michael Hohmann, Farina Kindermann, Tobias Lausch, Daniel Mayer, Felix Schmidt, and Artur Widera, "Single-atom thermometer for ultracold gases," Phys. Rev. A **93**, 043607 (2016).

[32] Cheng Chin, Rudolf Grimm, Paul Julienne, and Eite

Tiesinga, "Feshbach resonances in ultracold gases," Rev. Mod. Phys. **82**, 1225–1286 (2010).

[33] R. Dorner, S. R. Clark, L. Heaney, R. Fazio, J. Goold, and V. Vedral, "Extracting quantum work statistics and fluctuation theorems by single-qubit interferometry," Physical Review Letters **110**, 230601 (2013).

[34] L. Mazzola, G. De Chiara, and M. Paternostro, "Measuring the characteristic function of the work distribution," Phys. Rev. Lett. **110**, 230602 (2013).

[35] Tiago B. Batalhão, Alexandre M. Souza, Laura Mazzola, Ruben Auccaise, Roberto S. Sarthour, Ivan S. Oliveira, John Goold, Gabriele De Chiara, Mauro Paternostro, and Roberto M. Serra, "Experimental reconstruction of work distribution and study of fluctuation relations in a closed quantum system," Phys. Rev. Lett. **113**, 140601 (2014).

[36] Manuel Gessner, Michael Ramm, Hartmut Häffner, Andreas Buchleitner, and Heinz-Peter Breuer, "Observing a quantum phase transition by measuring a single spin," Europhys. Lett. **107**, 40005 (2014).

[37] Francesco Cosco, Massimo Borrelli, Francesco Plastina, and Sabrina Maniscalco, "Detection of superfluid excitations via local quantum probing," (2015), pre-print available at arXiv:1511.00833.

[38] T. H. Johnson, F. Cosco, M. T. Mitchison, D. Jaksch, and S. R. Clark, "Thermometry of ultracold atoms via nonequilibrium work distributions," Physical Review A **93**, 053619 (2016).

[39] T. J. Elliott and T. H. Johnson, "Nondestructive probing of means, variances, and correlations of ultracold-atomic-system densities via qubit impurities," Phys. Rev. A **93**, 043612 (2016).

[40] Jesper Levinsen, Meera M. Parish, and Georg M. Bruun, "Impurity in a Bose-Einstein condensate and the Efimov effect," Phys. Rev. Lett. **115**, 125302 (2015).

[41] P. Haikka, S. McEndoo, G. De Chiara, G. M. Palma, and S. Maniscalco, "Quantifying, characterizing, and controlling information flow in ultracold atomic gases," Phys. Rev. A **84**, 031602 (2011).

[42] Michael Streif, *Investigating ultracold atom systems using multiple quantum probes*, Master's thesis, U. Freiburg (2016).

[43] M. A. Nielsen, E. Knill, and R. Laflamme, "Complete quantum teleportation using nuclear magnetic resonance," Nature **396**, 52–55 (1998).

[44] D. Jaksch, C. Bruder, J. I. Cirac, C. W. Gardiner, and P. Zoller, "Cold Bosonic Atoms in Optical Lattices," Physical Review Letters **81**, 3108–3111 (1998).

[45] Markus Greiner, Olaf Mandel, Tilman Esslinger, Theodor W. Hänsch, and Immanuel Bloch, "Quantum phase transition from a superfluid to a Mott insulator in a gas of ultracold atoms," Nature **415**, 39–44 (2002).

[46] JH Huckans, IB Spielman, B Laburthe Tolra, WD Phillips, and JV Porto, "Quantum and classical dynamics of a Bose-Einstein condensate in a large-period optical lattice," Physical Review A **80**, 043609 (2009).

[47] Lev P. Pitaevskii and Sandro Stringari, *Bose-Einstein condensation* (Oxford University Press, 2003).

[48] Klaus Mayer, Alberto Rodriguez, and Andreas Buchleitner, "Matter-wave scattering from strongly interacting bosons in an optical lattice," Physical Review A **91**, 053633 (2015).

[49] Maciej Lewenstein, Anna Sanpera, and Verònica Ahufinger, *Ultracold Atoms in Optical Lattices: Simulating quantum many-body systems* (OUP, Oxford, 2012).

[50] Allan Griffin, "Conserving and gapless approximations for an inhomogeneous Bose gas at finite temperatures," Physical Review B **53**, 9341 (1996).

[51] Bogdan Damski and Jakub Zakrzewski, "Properties of the one-dimensional Bose-Hubbard model from a high-order perturbative expansion," New Journal of Physics **17**, 125010 (2015).

[52] C. Menotti, M. Krämer, L. P. Pitaevskii, and S. Stringari, "Dynamic structure factor of a Bose-Einstein condensate in a one-dimensional optical lattice," Physical Review A **67**, 053609 (2003).

[53] I. Bloch, J. Dalibard, and W. Zwerger, "Many-body physics with ultracold gases," Reviews of Modern Physics **80**, 885–964 (2008).

[54] P. Deuar, A. G. Sykes, D. M. Gangardt, M. J. Davis, P. D. Drummond, and K. V. Kheruntsyan, "Nonlocal pair correlations in the one-dimensional Bose gas at finite temperature," Physical Review A - Atomic, Molecular, and Optical Physics **79**, 043619 (2009).

[55] Anton Öttl, Stephan Ritter, Michael Köhl, and Tilman Esslinger, "Correlations and counting statistics of an atom laser," Physical Review Letters **95**, 090404 (2005).

[56] Martijn Schellekens, Rodolphe Hoppeler, Aurélien Perrin, J Viana Gomes, Denis Boiron, Alain Aspect, and Christoph I Westbrook, "Hanbury brown twiss effect for ultracold quantum gases," Science **310**, 648–651 (2005).

[57] Marco Anderlini, Patricia J. Lee, Benjamin L. Brown, Jennifer Sebby-Strabley, William D. Phillips, and J. V. Porto, "Controlled exchange interaction between pairs of neutral atoms in an optical lattice," Nature **448**, 452–456 (2007).

[58] Simon Fölling, Stefan Trotzky, Patrick Cheinet, Michael Feld, Robert Saers, Artur Widera, Torben Müller, and Immanuel Bloch, "Direct observation of second-order atom tunnelling," Nature **448**, 1029–1032 (2007).

[59] S Hofferberth, I Lesanovsky, B Fischer, T Schumm, and J Schmiedmayer, "Non-equilibrium coherence dynamics in one-dimensional Bose gases," Nature **449**, 324–327 (2007).

[60] Dominik Hangleiter, MT Mitchison, TH Johnson, M Bruderer, MB Plenio, and D Jaksch, "Nondestructive selective probing of phononic excitations in a cold bose gas using impurities," Physical Review A **91**, 013611 (2015).

[61] R. Orús, "Advances on tensor network theory: symmetries, fermions, entanglement, and holography," European Physical Journal B **87**, 280 (2014).

[62] S. Al-Assam, S. R. Clark, and D. Jaksch, "Tensor network theory," (2016), pre-print available at arXiv:1610.02244.

[63] S Al-Assam, S. R. Clark, D Jaksch, and TNT Development team, "Tensor Network Theory Library," (2015), beta version 1.0.13, www.tensornetworktheory.org.

[64] M. Endres, M. Cheneau, T. Fukuhara, C. Weitenberg, P. Schauß, C. Gross, L. Mazza, M. C. Bañuls, L. Pollet, I. Bloch, and S. Kuhr, "Single-site- and single-atom-resolved measurement of correlation functions," Applied Physics B **113**, 27–39 (2013).

[65] A Recati, PO Fedichev, W Zwerger, J Von Delft, and P Zoller, "Atomic quantum dots coupled to a reservoir of a superfluid Bose-Einstein condensate," Physical review

letters **94**, 040404 (2005).
[66] Eriko Kaminishi, Takashi Mori, Tatsuhiko N Ikeda, and Masahito Ueda, "Entanglement pre-thermalization in a one-dimensional Bose gas," Nature Physics **11**, 1050–1056 (2015).
[67] Asher Peres, "Stability of quantum motion in chaotic and regular systems," Physical Review A **30**, 1610 (1984).
[68] Rodolfo A. Jalabert and Horacio M. Pastawski, "Environment-independent decoherence rate in classically chaotic systems," Phys. Rev. Lett. **86**, 2490–2493 (2001).
[69] P. Haikka, J. Goold, S. McEndoo, F. Plastina, and S. Maniscalco, "Non-Markovianity, Loschmidt echo, and criticality: A unified picture," Physical Review A **85**, 060101 (2012).
[70] G Dattoli, J Gallardo, and A Torre, "Time-ordering techniques and solution of differential difference equation appearing in quantum optics," Journal of mathematical physics **27**, 772–780 (1986).
[71] Alfred Wunsche, "Displaced Fock states and their connection to quasiprobabilities," Quantum Optics: Journal of the European Optical Society Part B **3**, 359 (1991).
[72] G. Arfken, *Mathematical Methods for Physicists*, 3rd ed. (Academic Press, Orlando, FL, 1985).